environments

MDPI

Article

Partial Nitritation Under Zero-Pressure Aeration in a Membrane-Aerated Biofilm Reactor: Nitrite Accumulation, EPS Molecular Structure, and Microbial Community

Peishan Yang, Yu Cao, Peng Zheng *, Ying Liu, Mingxin Zhu, Hua Zhou and Shunlong Pan

School of Environmental Science and Engineering, Nanjing Tech University, Nanjing 211816, China; 202361202039@njtech.edu.cn (P.Y.); ly1074071123@163.com (Y.L.); zmx@njtech.edu.cn (M.Z.); zhouhua@njtech.edu.cn (H.Z.); shunlongpan@njtech.edu.cn (S.P.)

* Correspondence: zhengpeng1991@njust.edu.cn; Tel.: +86-25-5813-9652

Abstract

Achieving stable partial nitritation (PN) in mainstream municipal wastewater treatment is critical for energy-efficient anammox-based nitrogen removal. However, selectively suppressing nitrite-oxidizing bacteria (NOB) while retaining ammonia-oxidizing bacteria (AOB) remains challenging. This study investigated the performance and microbial mechanisms of PN in a membrane-aerated biofilm reactor (MABR) under zero-pressure aeration. The results showed that zero-pressure aeration achieved a nitrite accumulation ratio (NAR) of 82.14%, significantly higher than that under constant aeration (13.2%) and intermittent aeration (53.5%). Zero-pressure aeration led to a significant increase in the fluorescence intensities of tyrosine/tryptophan protein in extracellular polymeric substances. 16S rRNA sequencing revealed that zero-pressure aeration achieved a modest reduction in the relative abundance of NOB *Nitrospira* from 3.39% to 2.74% while increasing the relative abundance of AOB *Nitrosomonas* from 0.04% to 1.09%. Enzyme activity assays further showed that zero-pressure aeration significantly decreased nitrite oxidoreductase (NXR) activity while maintaining ammonia monooxygenase (AMO) and hydroxylamine oxidoreductase (HAO) activities, providing direct functional evidence for NOB suppression. Zero-pressure operation required no external air supply, representing a passive aeration strategy for PN. These results suggest that zero-pressure aeration may reshape the competition between AOB and NOB by enriching AOB and suppressing NOB, providing a new energy-efficient pathway for mainstream nitrogen removal.

Keywords: membrane aerated biofilm reactor; zero-pressure aeration; partial nitritation; extracellular polymeric substances; microbial community

Check for updates

Academic Editors: Simeone Chianese, Zhiqiang Zuo, Xiaoyuan Zhang and Xiaotong Cen

Received: 7 April 2026
Revised: 27 April 2026
Accepted: 29 April 2026
Published: 9 May 2026

Copyright: © 2026 by the authors. Licensee MDPI, Basel, Switzerland. This article is an open access article distributed under the terms and conditions of the Creative Commons Attribution (CC BY) license.

1. Introduction

Partial nitritation (PN), the biological oxidation of ammonium to nitrite without further oxidation to nitrate, is a prerequisite for energy-efficient nitrogen removal via the anammox process [1,2]. Compared with conventional nitrification–denitrification, PN can reduce aeration energy by approximately 25% and eliminate external carbon demand [3]. However, achieving stable PN in low-strength mainstream wastewater remains a major challenge, primarily due to the difficulty in selectively suppressing nitrite-oxidizing bacteria (NOB) while maintaining the activity of ammonia-oxidizing bacteria (AOB).

Membrane-aerated biofilm reactors (MABRs) have emerged as a promising platform for PN due to their unique counter-diffusion configuration, which creates steep oxygen

gradients within the biofilm [4,5]. By controlling the lumen pressure, oxygen supply can be regulated to suppress NOB effectively [6]. Recent studies have demonstrated that microbial activity can drive oxygen transfer across the membrane even under zero-pressure aeration, where membrane lumens are open to the atmosphere [7,8], suggesting the possibility of achieving PN without external aeration energy [9]. Nevertheless, the biofilm structure (extracellular polymeric substance, EPS) and microbial community responses under zero-pressure aeration have not been comprehensively investigated.

This study aimed to compare the PN performance of an MABR under constant, intermittent, and zero-pressure aeration modes, and to elucidate the microbial mechanisms by analyzing shifts in the biofilm structure and microbial community via fluorescence spectrometry and16S rRNA sequencing.

2. Materials and Methods

2.1. Membrane Aerated Biofilm Reactor

A laboratory-scale MABR was used for the partial nitritation experiments. The reactor was made of plexiglass with an effective volume of 2.0 L, an inner diameter of 9 cm, and a height of 55 cm. A water bath jacket was installed on the outer layer to maintain constant temperature. The membrane module consisted of polydimethylsiloxane (PDMS) hollow fiber membranes (Suwang Co., Ltd., Yancheng, China). Each membrane fiber had an outer diameter of 1.0 mm, an inner diameter of 0.5 mm, and an effective length of 0.35 m. Each membrane module contained 850 fibers, providing a total membrane surface area of 0.93 m^2 and a specific surface area of 465 $m^2 \cdot m^{-3}$. The membrane module was assembled in a dead-end configuration (Figure 1). Air was supplied through the membrane lumen, with the aeration pressure controlled by a pressure gauge and adjusted by an exhaust valve. The reactor was operated in continuous-flow mode, with wastewater entering from the bottom and exiting from the top. The hydraulic retention time (HRT) was controlled by a peristaltic pump. An internal recirculation from top to bottom was installed to promote mixing uniformity within the reactor. More detailed properties of the PDMS membrane used in this study are shown in Table S1.

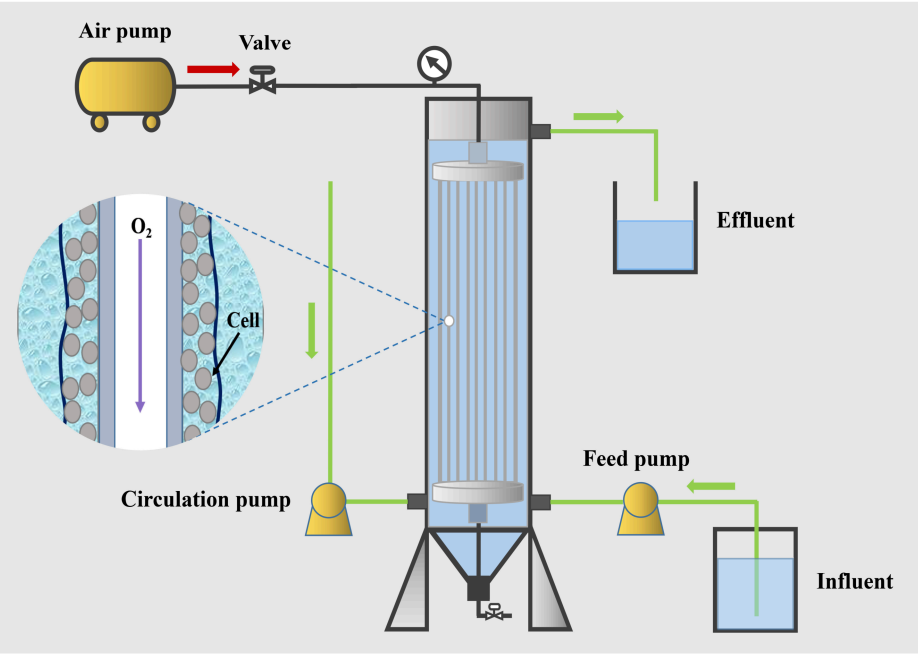


Figure 1. Schematic diagram of the reactor. (The arrow indicates the direction of water flow.)

2.2. Experimental Procedures

The reactor was inoculated with activated sludge taken from the nitrification tank of an industrial wastewater treatment plant. The sludge exhibited certain toxicity tolerance and high nitrification activity. Prior to inoculation, 500 mL of activated sludge was mixed with 1.5 L of synthetic ammonium wastewater with an NH_4^+-N concentration of 50 mg·L^{-1} at pH 7.0, and the mixture was added to the reactor. The initial aeration pressure was set at 0.01 MPa, and internal recirculation was operated for 48 h to promote sludge attachment onto the membrane surface. Subsequently, continuous feeding started with an HRT of 48 h. After two weeks of operation, suspended sludge was discharged, and the membrane surface turned yellow, indicating successful biofilm formation. Thereafter, the HRT was gradually adjusted to 24 h and the aeration pressure to 5 kPa, and the reactor was acclimated until complete oxidation of ammonium was achieved, marking the completion of the preliminary start-up of the reactor.

To investigate the effects of aeration mode on partial nitritation performance and microbial community structure, three aeration modes were compared in this study: constant-pressure aeration, with the membrane lumen pressure maintained at 5 kPa; intermittent aeration, with each aeration cycle of 12 h consisting of 6 h of aeration followed by 6 h without aeration; and zero-pressure aeration, with the inlet ends of the membrane fibers directly open to the atmosphere and no external pressure applied. In all stages, the influent NH_4^+-N concentration was maintained at 50 mg·L^{-1}, the pH was adjusted to 8.0, the HRT was set at 24 h, and the temperature was controlled at 35 ± 1 °C. The membrane module was backwashed every 14 days to control excessive biofilm growth. The operational parameters at different stages of partial nitritation start-up are shown in Table S2.

2.3. Analytical Methods

Water samples were filtered through 0.22 μm membrane filters before analysis. NH_4^+-N was determined using Nessler's reagent spectrophotometry (HJ 535-2009). NO_2^--N was determined using N-(1-naphthyl)-ethylenediamine spectrophotometry (GB/T 7493-1987). NO_3^--N was determined using thymol spectrophotometry. Dissolved oxygen (DO) concentration was measured using a portable dissolved oxygen meter (Multi 3620 IDS, WTW, Weilheim, Germany), and pH was measured using a pH meter (FE28, Mettler Toledo, Columbus, OH, USA). The nitrite accumulation ratio (NAR) was calculated according to the following formula (Equation (1)). The reactor was operated in continuous-flow mode throughout the experiment. Under each operating condition, the reactor was run stably for at least three hydraulic retention times before data collection. The NAR was calculated using Equation (1) based on the measured concentrations of NO_2^--N and NO_3^--N. For DO, pH, and EPS protein/polysaccharide contents, triplicate measurements were performed, and data are presented as mean ± standard deviation. Statistical comparisons among different aeration modes were performed using one-way analysis of variance (ANOVA) followed by Tukey's post hoc test, with a significance level of $p < 0.05$.

$$NAR = [NO_2^-\text{-N}]/([NO_2^-\text{-N}] + [NO_3^-\text{-N}]) \times 100\% \quad (1)$$

3. Results and Discussion

3.1. Start-Up of the MABR for Partial Nitritation

Preliminary experiments aimed to optimize operational conditions for achieving partial nitritation with a high ammonium conversion rate. As shown in Figure 2, during the first 13 days, HRT was set at 48 h and 24 h with an aeration pressure of 10 kPa. Ammonium was completely converted to nitrate, indicating sufficient oxygen supply or long HRT. On day 14, HRT was reduced to 12 h, resulting in nitrite accumulation of 1.26 mg·L^{-1} and a

NAR of 7%, but ammonium conversion was low with effluent NH_4^+ of 29.58 mg·L^{-1}. An HRT of 24 h was eventually selected to balance the conversion rate and NAR. From day 21 to 34, influent pH was increased stepwise from 7.0 to 8.0. Effluent NH_4^+ remained below 3 mg·L^{-1}, and NAR gradually increased with pH, reaching 5.23% at pH 8.0. On day 35, aeration pressure was reduced to 5 kPa, and effluent NH_4^+ increased to 6.46 mg·L^{-1}, suggesting microbial adaptation to low DO. By day 38, NH_4^+ was fully consumed, but NAR did not increase, indicating successful adaptation. According to Pellicer-Nàcher et al. [10], under zero pressure, atmospheric oxygen is drawn into the membrane lumen by the pressure gradient created by microbial oxygen metabolism. In this study, after two cycles under zero pressure, effluent NH_4^+ decreased to 3.12 mg·L^{-1} and NAR increased to 11.37%, demonstrating that this strategy enhanced nitrite accumulation while maintaining high ammonium conversion. On day 49, influent NH_4^+ was increased to 70 mg·L^{-1} to enhance treatment capacity and increase free ammonia for NOB suppression. From day 49 to 56, NAR increased from 17.76% to 34.14%. On day 57, HRT was shortened to 12 h to further increase NAR and potentially wash out NOB. On day 66, NAR reached 74.07% with effluent nitrite of 30.26 mg·L^{-1}, but effluent NH_4^+ was high at 27.35 mg·L^{-1}. Over time, ammonium conversion increased while NAR decreased. By day 75, the reactor stabilized with effluent NH_4^+ of 20.64 mg·L^{-1} and NAR around 66%. The decreasing effluent NH_4^+ suggested AOB growth, indicating that zero-pressure conditions could meet AOB oxygen demand.

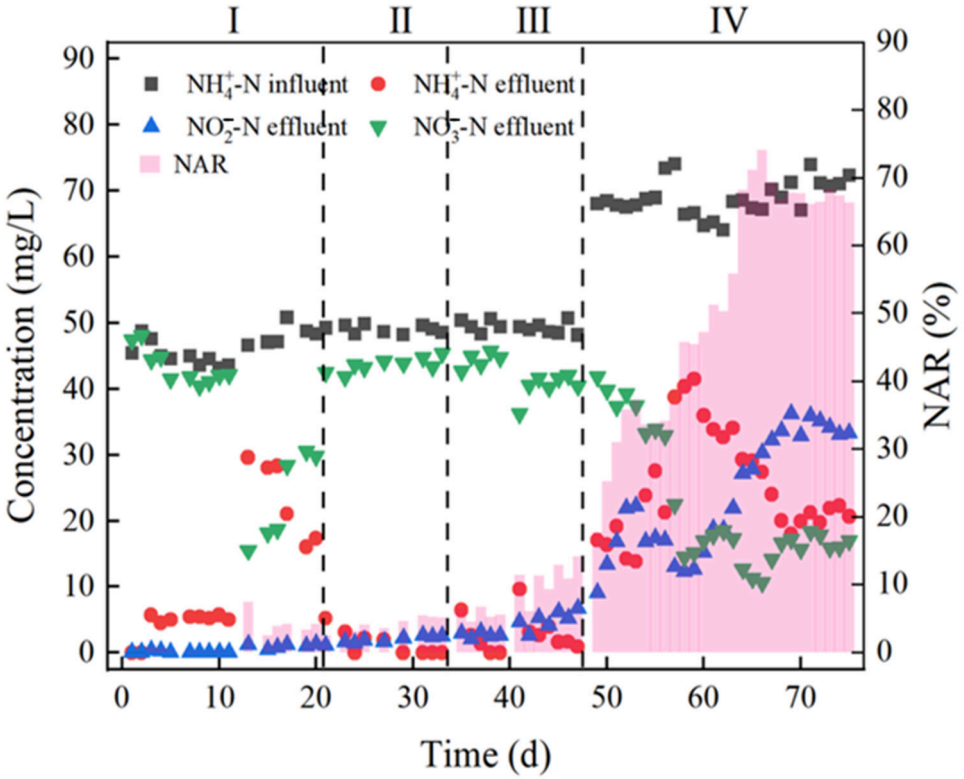


Figure 2. NH_4^+-N, NO_2^--N, NO_3^--N concentrations and NAR in the reactor during start-up. Vertical dashed lines separate different operational phases: I (HRT adjustment), II (pH increase from 7.0 to 8.0), III (aeration pressure reduction from 10 kPa to zero-pressure), and IV (influent NH_4^+-N increase to 70 mg/L and HRT reduction).

As shown in Figure 2, pH and aeration pressure were the key factors affecting NAR. At 5 kPa, 50 mg·L^{-1} NH_4^+ was completely nitrified. According to Chen et al. [11], intermittent aeration effectively achieves partial nitritation. Therefore, further investigation

was conducted to elucidate the mechanisms by which pH and aeration mode influence partial nitritation.

3.2. Influence of Influent pH on Partial Nitritation Performance

3.2.1. Performance of the Reactor Under Different pH Conditions

As shown in Figure 3, the influent and effluent concentrations of NH_4^+-N, NO_2^--N, and NO_3^--N, as well as NAR, dissolved oxygen concentration in the reactor, and influent and effluent pH values, are presented for influent pH values of 7.0, 7.5, and 8.0. At pH 7.0, with an aeration pressure of 5 kPa, HRT of 24 h, and influent NH_4^+-N concentration of 50 mg·L^{-1}, the reactor operated under complete nitrification. The average effluent NO_2^--N concentration was 0.47 ± 0.19 mg·L^{-1}, and the average effluent NO_3^--N concentration was 48.29 ± 1.08 mg·L^{-1}, with NAR decreasing to below 1.5%. This was likely because the relatively low pH favored NOB growth, resulting in high NOB activity and unrestricted nitrite conversion. Under conditions of sufficient dissolved oxygen and favorable pH, NOB could quickly recover their activity, promoting complete nitrification [12]. On day 17, the influent pH was increased to 7.5. NAR suddenly rose to 8.91%, with an effluent NO_2^--N concentration of 4.53 mg·L^{-1}. However, as operation continued, NAR decreased to 2.79% and remained relatively stable. After the pH increase, NOB were inhibited to some extent, but over time, they gradually adapted to the higher-pH environment. On day 35, the influent pH was further increased to 8.0. NAR showed significant accumulation and gradually increased, reaching 17.07% on day 42, after which it remained relatively stable. At an influent pH of 8.0, AOB growth was favored, while NOB could not adapt well and were gradually outcompeted. As NAR increased, the dissolved oxygen concentration in the reactor correspondingly increased (Figure 4a). Nitrifying bacteria consumed alkalinity during ammonium oxidation, leading to a decrease in pH (Figure 4b).

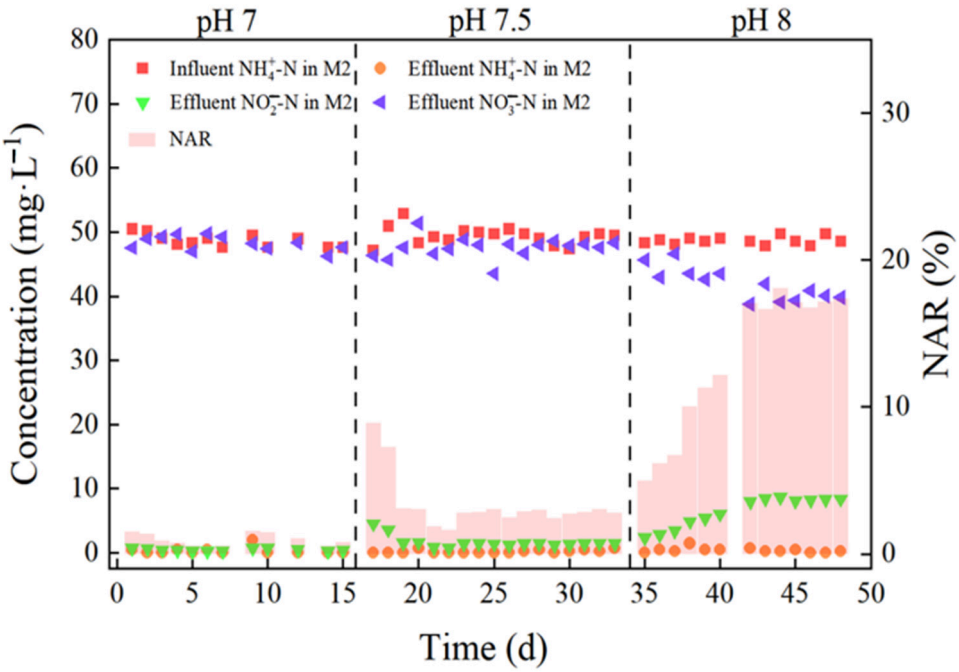


Figure 3. NH_4^+-N, NO_2^--N, NO_3^--N concentrations and NAR in the reactor at different pH values.

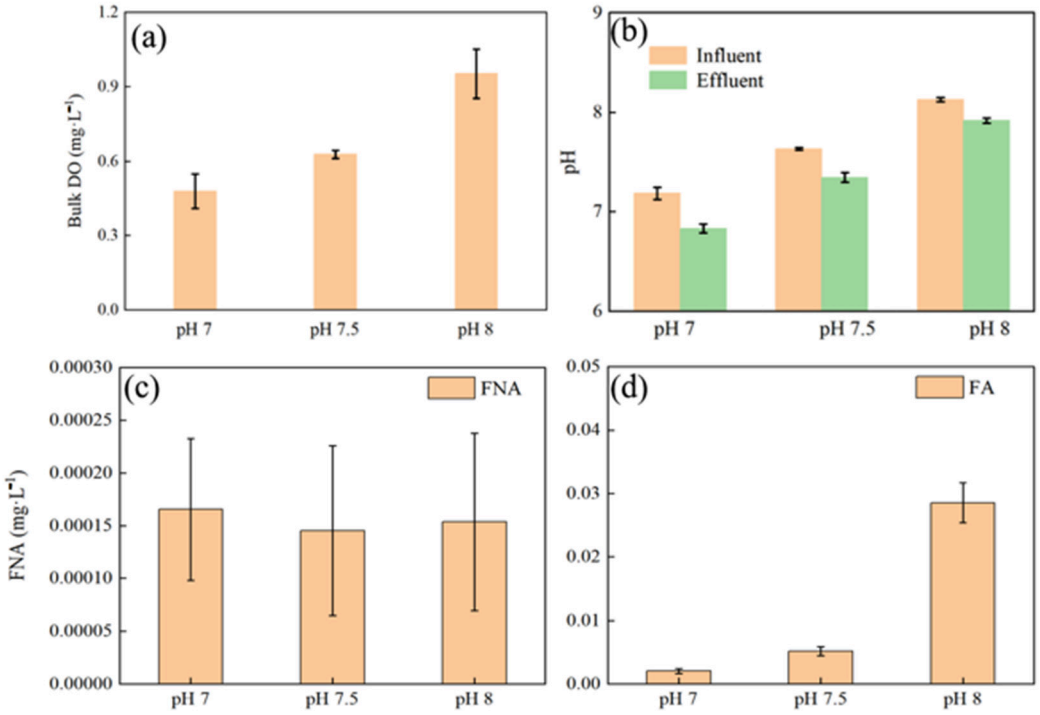


Figure 4. DO concentration (**a**), influent/effluent pH (**b**), FNA (**c**), and FA (**d**) in the reactor at different pH values.

The effect of pH on partial nitritation is manifested in two aspects. On the one hand, AOB and NOB have different optimal pH ranges, and pH affects the enzymes of nitrifying bacteria [13,14]. On the other hand, pH influences the concentrations of free ammonia (FA) and free nitrous acid (FNA), which are both substrates for the nitrification process and inhibitors of AOB and NOB [15]. The FA and FNA concentrations in the reactor effluent were calculated. As shown in Figure 4c,d, the effluent FA and FNA concentrations were low, and based solely on the inhibitor concentrations in the effluent, it could not be inferred that they inhibited NOB. This observation is consistent with previous reports. Chen et al. demonstrated that the increase in FA concentration at elevated pH contributes to NOB suppression, as NOB are more susceptible to FA inhibition than AOB [12]. However, in this study, the calculated FA and FNA concentrations were below the reported inhibition thresholds, suggesting that direct pH effects on enzyme activity may play a more important role than FA/FNA inhibition under the tested conditions [16]. Furthermore, Wang et al. showed that limiting the oxygen concentration in the inner biofilm and the thickness of the aerobic biofilm is key to NOB suppression, and pH regulation can further enhance this effect [17].

3.2.2. Characterization of EPS in the Nitrifying Biofilm Under Different Aeration Modes

Although EPS lacks metabolic activity, it plays a crucial role in cell aggregation, stress protection, and the construction and maintenance of biofilm structure while also influencing overall system performance. The tightly bound EPS (TB-EPS) and loosely bound EPS (LB-EPS) that are secreted by the attached microorganisms control biofilm formation; therefore, their study is of critical importance. The components of the biofilm were characterized using three-dimensional fluorescence spectroscopy (Figure S1). LB-EPS exhibited three fluorescence peaks, designated as peaks B, C, and D. The most intense peak B was identified as a tyrosine/tryptophan protein peak [18]. According to Xu et al. [19], peak C is associated with humic acid-like substances, and peak D is a characteristic peak of fulvic acid. TB-EPS exhibited two fluorescence peaks, designated as peaks A and B. Peak A is associated with

aromatic proteins [20]. As the influent pH increased, the composition of EPS in the biofilm remained unchanged, but the fluorescence intensities of the peaks changed. Notably, when the NAR reached 17%, the fluorescence intensities of the protein peaked in both LB-EPS and TB-EPS, and the humic acid- and fulvic acid-related peaks in LB-EPS increased significantly. Nitrite has been shown to effectively lyse microbial cell walls, thereby enhancing hydrolysis efficiency [21]. Furthermore, proteins are the main components of the biofilm, and an increase in protein content helps the biofilm resist external toxic stress. The accumulation of nitrites likely contributed to the increased fluorescence intensity of the protein peaks. Zhou also observed a significant increase in TB-EPS protein content in nitritation activated sludge under ambient-temperature conditions [22]. The peaks related to fulvic acid and humic acid appeared only in LB-EPS, which is consistent with the EPS results reported by Xu for partial nitritation biofilms [19]. The fluorescence intensity of the tryptophan protein peak in TB-EPS was much higher than that in LB-EPS, and an aromatic protein peak appeared in TB-EPS, likely because tightly bound EPS primarily relies on proteins to maintain biofilm structure. The EPS characteristics of the nitrifying biofilm in this study are consistent with the findings of the above studies, indicating the gradual achievement of partial nitritation in this experimental system.

Figure 5a,b show the protein and polysaccharide contents in EPS under different pH conditions, respectively. As the influent pH increased, both protein and polysaccharide contents in EPS increased correspondingly. The protein content in TB-EPS increased from 18.73 mg·g VSS^{-1} to 20.33 mg·g VSS^{-1}, and the protein content in LB-EPS increased from 10.39 mg·g VSS^{-1} to 21.33 mg·g VSS^{-1}. The polysaccharide content in TB-EPS increased from 4.34 mg·g VSS^{-1} to 5.55 mg·g VSS^{-1}, and the polysaccharide content in LB-EPS increased from 2.35 mg·g VSS^{-1} to 3.84 mg·g VSS^{-1}. The increase in EPS secretion by microorganisms was likely caused by nitrite accumulation. Nitrite is toxic to microorganisms, and its accumulation can inhibit the metabolism of several groups of bacteria involved in nitrogen removal in wastewater treatment plants [23]. Wilén et al. reported that increasing pollutant loading led to increased protein and polysaccharide contents in EPS [24]. Previous studies have also shown that both protein and polysaccharide contents increase during the achievement of partial nitritation [25]. Although the limited number of pH conditions precludes robust statistical correlation, a consistent trend was observed: as pH increased from 7.0 to 8.0, both TB-EPS protein content and NAR increased concomitantly. This trend suggests a potential association between EPS protein secretion and nitrite accumulation during PN establishment. The increase in EPS protein content under PN conditions may be attributed to two possible mechanisms. First, as reported by Sun et al. [26], proteins rather than polysaccharides play a key role in biofilm responses to environmental stress in MABR systems, and their secretion can be an active defense strategy against nitrite toxicity. Second, nitrite accumulation has been shown to induce microbial cell lysis, thereby releasing intracellular proteins into the EPS matrix [21]. In this study, the simultaneous increase in both TB-EPS and LB-EPS protein content suggests that both mechanisms may be involved. It is important to note that the observed increase in EPS protein content was concomitant with the increase in NAR, which suggests a potential association rather than a direct causal relationship. Whether the EPS protein increase actively contributes to PN stability or is merely a passive response to nitrite-induced stress requires further investigation. Nevertheless, the consistent trend observed under both pH variation and aeration mode shifts supports a potential link between EPS protein secretion and biofilm adaptation to nitrite accumulation. The NAR and EPS data indicated that partial nitritation performance gradually improved with increasing pH. Therefore, to achieve better partial nitritation performance, a relatively high pH of 8.0 was selected for further investigation of the effect of different aeration modes on partial nitritation.

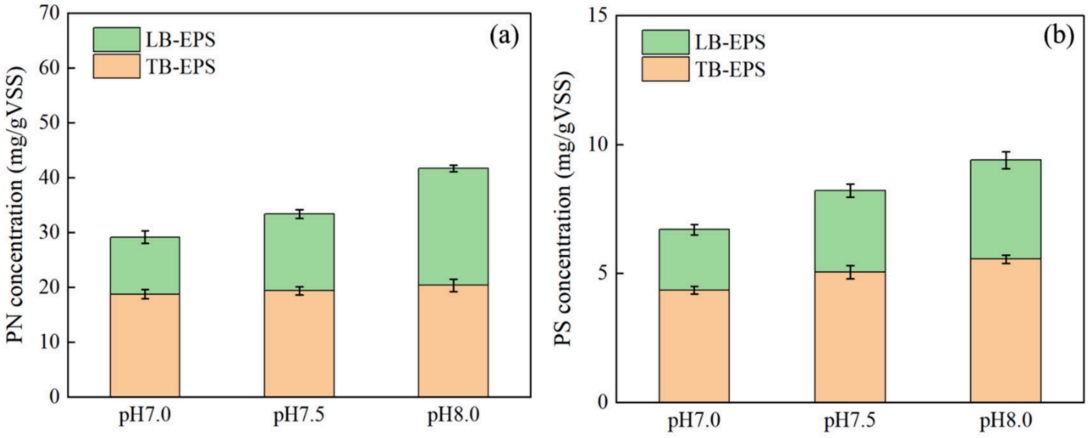


Figure 5. EPS composition of the biofilm under different influent pH conditions: (**a**) protein (PN) and (**b**) polysaccharide (PS).

3.3. Influence of Aeration Mode on Partial Nitritation Performance

3.3.1. Performance of the Reactor

As shown in Figure 6, the effects of constant-pressure aeration, intermittent aeration, and zero-pressure aeration on partial nitritation were investigated at pH 8.0 with an influent ammonium concentration of 50 mg·L^{-1}. Under intermittent and zero-pressure aeration, the NAR was significantly improved. During constant-pressure aeration, the average effluent ammonium concentration was 0.39 ± 0.38 mg·L^{-1}, the average effluent nitrite concentration was 6.39 ± 2.26 mg·L^{-1}, and the average NAR was 13.22 ± 4.68%. Under intermittent aeration, the average effluent ammonium concentration increased to 3.75 ± 1.82 mg·L^{-1}, the average effluent nitrite concentration increased to 17.52 ± 5.14 mg·L^{-1}, and the average NAR increased to 39.55 ± 9.77%. Under zero-pressure aeration, the average effluent ammonium concentration decreased to 2.42 ± 1.97 mg·L^{-1} compared to intermittent aeration, the average effluent nitrite concentration increased to 31.28 ± 4.81 mg·L^{-1}, and the average NAR was 68.25 ± 9.89%. According to Chen et al., a lumen pressure of 5 kPa is used for achieving partial nitritation in MABRs [12]. However, in this study, constant-pressure aeration at 5 kPa resulted in complete ammonium conversion, but the maximum NAR was only 17.39%. Intermittent aeration has been demonstrated as an effective strategy for achieving partial nitritation [11]. As shown in Figure 6, intermittent aeration effectively increased the NAR. After switching to this aeration strategy, the NAR rapidly increased to 26.24% and further increased with operation time, reaching 53.50% on day 58. Studies have shown that during the anoxic phase of intermittent aeration, NOB are more susceptible to inhibition, and when aeration is resumed, AOB recover their activity faster than NOB, leading to rapid nitrite accumulation [27]. Subsequently, the NAR gradually decreased and stabilized at 42.95%, which might be attributed to the gradual adaptation of NOB to the fluctuating dissolved oxygen environment [28]. It has been reported that when hollow fiber membranes are open to the atmosphere, microorganisms can drive oxygen transfer and thus achieve ammonium conversion [11,12]. AOB and NOB have different oxygen affinities, with AOB being more competitive under low-dissolved-oxygen conditions. Therefore, zero-pressure aeration provides favorable conditions for AOB survival. As shown in Figure 6, under zero-pressure aeration, not only was the effluent ammonium concentration very low, but the NAR further increased, eventually reaching 82.14%. According to Rosso et al., aeration energy accounts for 75% of the total energy consumption in wastewater treatment plants [29]. Under zero-pressure conditions, simply connecting the inlet ends of the hollow fiber membranes to the atmosphere enabled the conversion of 50 mg·L^{-1} of ammonium to nitrite or nitrate, demonstrating that the mechanism of partial nitritation in MABRs under

zero-pressure aeration is worthy of further exploration. In this study, both intermittent and zero-pressure aeration improved partial nitritation performance. Intermittent aeration rapidly increased the NAR in a short time, while zero-pressure aeration might be more advantageous for long-term NAR improvement and maintenance.

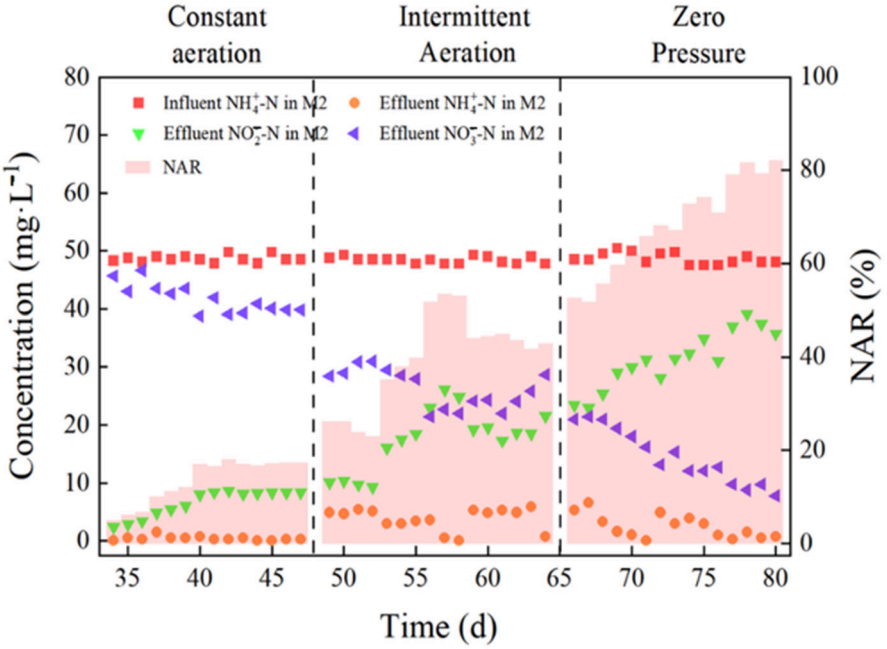


Figure 6. NH_4^+-N, NO_2^--N, NO_3^--N concentrations and NAR in the reactor under different aeration modes.

As shown in Figure 7a, the dissolved oxygen concentration in the reactor was 0.95 ± 0.10 mg·L^{-1} under constant-pressure aeration. Under intermittent aeration, due to reduced aeration time, the dissolved oxygen concentration decreased to 0.27 ± 0.08 mg·L^{-1}. Under zero-pressure aeration, the dissolved oxygen concentration further decreased to 0.12 ± 0.01 mg·L^{-1}. The improvement in partial nitritation performance was likely related to the decrease in dissolved oxygen. Because AOB have a higher oxygen affinity than NOB, they are more competitive than NOB under low-dissolved-oxygen conditions, thus favoring nitritation [30]. It should be recognized that this extremely low DO is the very essence of the zero-pressure aeration strategy. Without external pressure, microbial activity naturally creates an oxygen-limited environment [10]. At 0.12 mg·L^{-1}, the DO falls below the half-saturation coefficient of typical NOB (1.0–2.0 mg·L^{-1}) but remains within the range of AOB (0.3–0.6 mg·L^{-1}) [22], thereby selectively suppressing NOB. Similar observations have been reported under zero or ultra-low lumen pressure [31]. In summary, the aeration mode determines the pattern of oxygen supply, while the resulting DO concentration serves as the direct selective pressure that shapes the competition between AOB and NOB. Zero-pressure aeration is effective precisely because it passively creates and maintains an extremely low DO environment (0.12 mg/L) that favors AOB over NOB, without the need for active control of aeration cycles. Intermittent aeration, in contrast, relies on periodic anoxic disturbances to suppress NOB but requires precise cycle control. When the aeration mode was changed, the effluent pH remained stable at approximately 7.98 (Figure 7b). As shown in Figure 7c,d, the effluent FNA concentration gradually increased, which was associated with the increase in effluent nitrite concentration. The effluent FA concentration was highest under intermittent aeration because the effluent ammonium concentration was highest at this stage. However, both FA and FNA concentrations remained low and were insufficient to inhibit NOB. Nitrite is converted to FNA under acidic conditions but exists

as nitrite ions under alkaline conditions. It has been reported that nitrite has a greater toxic effect on sludge cells than FNA [32]. According to Sijbesma et al., nitrite ions increase the proton permeability of cell membranes, inhibit adenosine triphosphate (ATP) synthesis, and stimulate ATP hydrolysis [33]. Nitrite nitrogen concentrations of 5 to 40 mg·L^{-1} can cause inhibition [34]. Therefore, a higher nitrite concentration favors the maintenance of stable partial nitritation. From the perspective of aeration strategy, applying intermittent aeration first to rapidly increase nitrite accumulation, followed by further reducing the dissolved oxygen concentration in the reactor, can accelerate the improvement of partial nitritation performance and benefit its long-term maintenance [35].

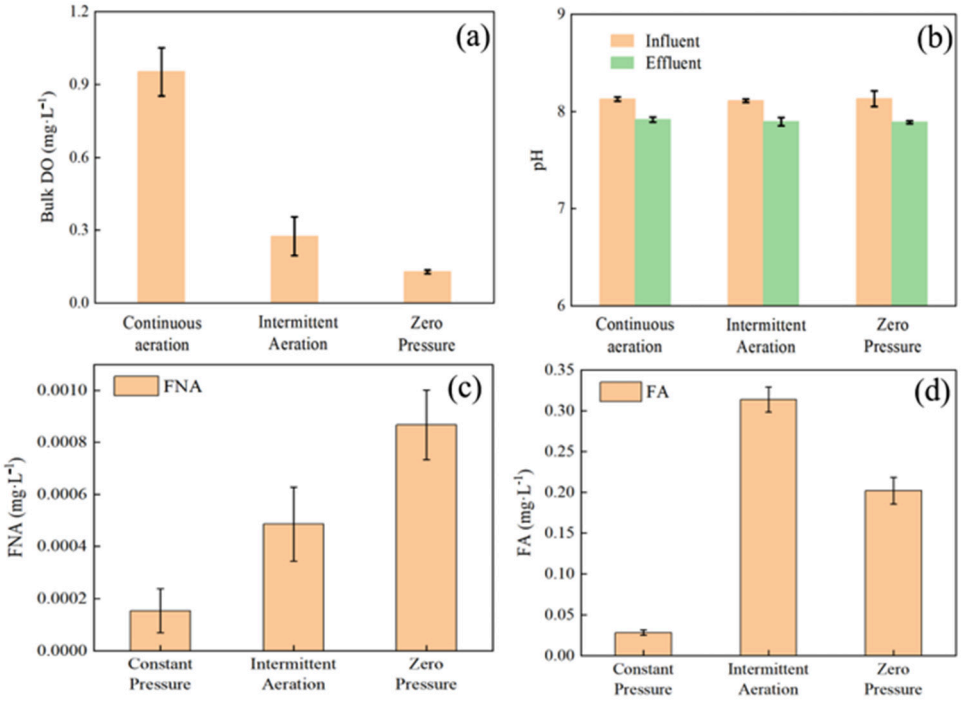


Figure 7. DO concentration (**a**), influent/effluent pH (**b**), FNA (**c**), and FA (**d**) in the reactor under different aeration conditions.

3.3.2. Characterization of EPS in the Nitrifying Biofilm

The components of the biofilm under different aeration modes were characterized using three-dimensional fluorescence spectroscopy (Figure S2). Consistent with Figure S1, LB-EPS exhibited three fluorescence peaks: a tyrosine/tryptophan protein peak, a peak associated with humic acid-like substances, and a characteristic peak of fulvic acid. TB-EPS exhibited two fluorescence peaks: an aromatic protein-related peak and a tyrosine/tryptophan protein peak. When the aeration mode was changed from constant-pressure aeration to intermittent aeration and then to zero-pressure aeration, the composition of EPS in the biofilm remained unchanged, but the fluorescence intensities of the peaks changed. Notably, as NAR increased, the fluorescence intensities of the protein peaks in both LB-EPS and TB-EPS, as well as the humic acid- and fulvic acid-related peaks in LB-EPS, increased significantly. The reasons for the increase in proteinaceous and humic substances were partially consistent with those described in Section 3.2.2. The increase in nitrite led to microbial cell lysis, which promoted the secretion of humic-like substances. Additionally, the biofilm secreted more proteins to defend against external environmental stress. Besides the stress caused by increased nitrite concentration, the reduction or fluctuation in dissolved oxygen induced by intermittent and zero-pressure aeration also inhibited AOB and NOB. When dissolved oxygen decreased, AOB and NOB tended to grow in the inner layers of the biofilm to access more oxygen and occupy favorable ecological niches. This likely

prompted microorganisms to secrete more TB-EPS to strengthen the biofilm structure and anchor their position.

As shown in Figure 8a,b, under intermittent and zero-pressure aeration, the protein content in TB-EPS increased significantly from 20.33 ± 1.16 mg·g VSS^{-1} to 22.33 ± 0.44 mg·g VSS^{-1} and to 34.98 ± 0.65 mg·g VSS^{-1}, respectively. Under intermittent aeration, the polysaccharide content in TB-EPS increased from 5.55 ± 0.16 mg·g VSS^{-1} to 6.35 ± 0.35 mg·g VSS^{-1}, and the polysaccharide content in LB-EPS increased from 3.84 ± 0.32 mg·g VSS^{-1} to 4.39 ± 0.29 mg·g VSS^{-1}. Under zero-pressure aeration, the polysaccharide content in TB-EPS showed little change, while the polysaccharide content in LB-EPS increased to 5.36 ± 0.16 mg·g VSS^{-1}. During the increase in nitrite concentration, both protein and polysaccharide contents in the biofilm EPS exhibited an upward trend, indicating favorable partial nitritation performance. Similarly, under different aeration modes, a consistent trend was observed: as aeration shifted from constant to intermittent to zero-pressure, both TB-EPS protein content and NAR increased. This trend further supports the potential role of EPS protein secretion in biofilm adaptation to nitrite accumulation and oxygen limitation. As discussed above, the increase in protein content may reflect both active defense against environmental stress [26] and passive release due to nitrite-induced cell lysis [21]. It is also important to note that this concomitant increase in TB-EPS protein content and NAR under different aeration modes suggests an association rather than a direct causal relationship. Further studies are needed to elucidate whether the EPS protein increase actively contributes to PN stability or primarily reflects a passive response to nitrite-induced stress. Both intermittent aeration and zero-pressure aeration have high application value. Zero-pressure aeration may be more suitable for mainstream wastewater with low ammonium loading, while intermittent aeration can be applied to treat wastewater with high ammonium loading by further adjusting the aeration frequency and aeration pressure. In practical applications, the choice of aeration mode should be based on the pollutant loading to maintain a high ammonium conversion rate and a high NAR.

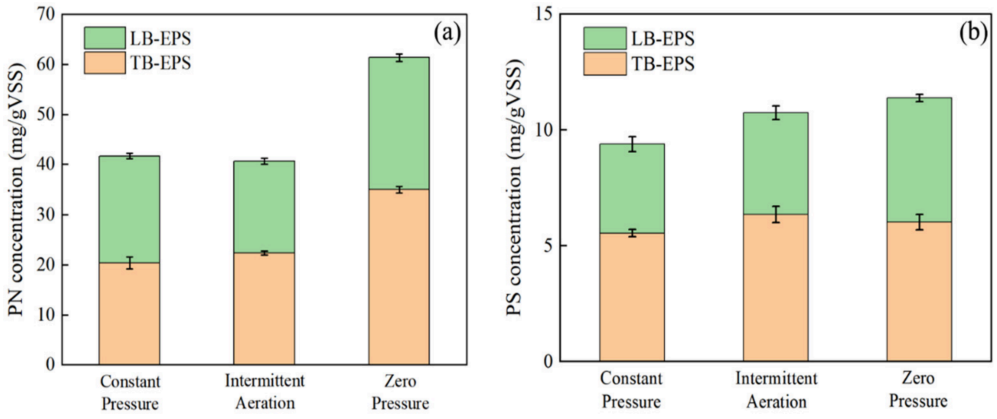


Figure 8. EPS composition of the biofilm under different aeration conditions: (**a**) protein (PN) and (**b**) polysaccharide (PS).

3.4. Community Structure of the Nitrifying Biofilm for Partial Nitritation

High-throughput sequencing was used to analyze the changes in microbial community structure in the biofilm under different aeration modes. As shown in Figure 9a, at the phylum level, the microbial community was dominated by Chloroflexi, Bacteroidota, Proteobacteria, Acidobacteriota, Firmicutes, Actinobacteriota, and Nitrospirota, with final relative abundances of 38.02%, 13.32%, 12.83%, 12.75%, 6.90%, 4.89%, and 2.74%, respectively. Chloroflexi is a functional bacterium that contributes to the structural integrity of the biofilm [36].

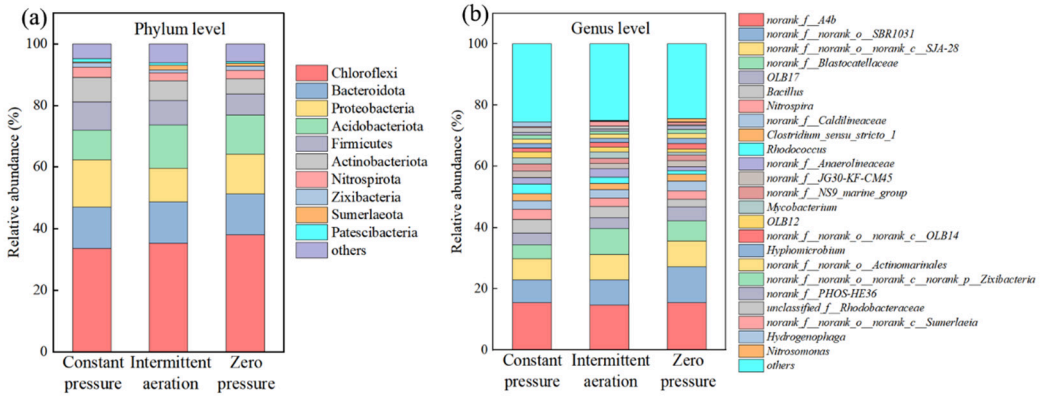


Figure 9. Microbial community structure of the reactor biofilm at the phylum level (**a**) and genus level (**b**) under constant-pressure, intermittent, and zero-pressure aeration.

As shown in Figure 9b, at the genus level, *norank_f_A4b*, *norank_f_norank_o_SBR1031*, *norank_f_norank_o_norank_c_SJA-28*, *norank_f_Blastocatellaceae*, *OLB17*, *Bacillus*, and *Nitrospira* were dominant in biofilm. *norank_f_A4b* and *norank_f_norank_o_SBR1031* can degrade complex macromolecular organic compounds [37]. *norank_f_A4b* typically grows in anaerobic environments and has a higher proportion outside the biofilm than inside [38]. Unclassified *SJA-28*, belonging to *Bacteroidota*, is a denitrifying bacterium capable of COD removal and nitrogen removal [39]. *norank_f_Blastocatellaceae* can also metabolize complex organic compounds [40]. Due to the low oxygen supply under different aeration modes, the dissolved oxygen concentration in the reactor remained at a low level, and an anaerobic zone formed outside the biofilm, providing a suitable environment for anaerobic microorganisms [41]. This led to varying degrees of increase in the relative abundances of the aforementioned genera. The relative abundances of *norank_f_norank_o_SBR1031*, *SJA-28*, and *norank_f_Blastocatellaceae* increased from 7.42%, 6.96%, and 4.55% to 11.77%, 8.36%, and 6.56%, respectively. The relative abundances of nitrifying genera in the biofilm varied under different aeration modes. Under constant-pressure aeration, intermittent aeration, and zero-pressure aeration, the relative abundances of *Nitrospira* were 3.39%, 2.69%, and 2.74%, respectively; those of *norank_f_JG30-KF-CM45* were 2.10%, 1.68%, and 2.10%, respectively; those of *norank_f_NS9_marine_group* were 2.27%, 1.59%, and 1.74%, respectively; those of *OLB12* were 1.99%, 1.62%, and 1.10%, respectively; and those of *Nitrosomonas* were 0.04%, 0.09%, and 1.09%, respectively. *Nitrospira* is a common NOB widely distributed in nature [1]. It has been reported that *norank_f_NS9_marine_group* possesses ammonia-oxidizing function and is an AOB [36]. *Nitrosomonas* is a typical AOB that converts ammonium to nitrite [42]. *norank_f_JG30-KF-CM45* belongs to *Chloroflexi* and is a nitrifying bacterium [43]. Li et al. found that *OLB12* participates in the nitrification process in wastewater treatment [44]. Under intermittent and zero-pressure aeration conditions, the relative abundances of all nitrifying bacteria, except for *Nitrosomonas*, decreased to some extent. This phenomenon may be attributed to the fact that low dissolved oxygen is unfavorable for the growth of nitrifying bacteria. In addition, intermittent aeration caused pH fluctuations within the biofilm, inhibiting the activity of nitrifying bacteria, especially NOB, resulting in lower relative abundances of nitrifying bacteria under this condition [45]. AOB have a higher oxygen affinity coefficient and a wider suitable pH range, allowing them to survive better under low-dissolved-oxygen conditions. Therefore, the relative abundance of *Nitrosomonas* increased continuously with reactor operation. Since most nitrifying bacteria, especially NOB, were inhibited and their abundances decreased, while some AOB remained active under intermittent and non-aeration conditions and their abundances increased, the NAR increased and partial nitritation was achieved. Among the three aeration modes, constant-pressure aeration provided sufficient dissolved oxygen

within the biofilm, favoring NOB growth; intermittent aeration had a stronger inhibitory effect on NOB; and zero-pressure aeration was more favorable for AOB growth [46].

3.5. Enzyme Activities of Nitrification Pathways

To further investigate the functional basis of PN achievement, the activities of key nitrification enzymes—AMO, HAO, and NXR—were determined. The results are presented in Figure 10.

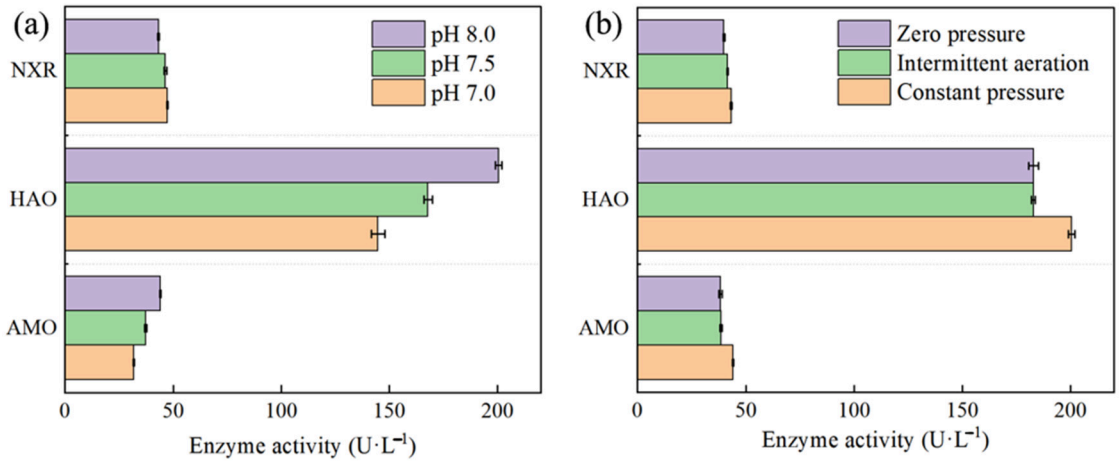


Figure 10. Nitrification enzyme activities under different pH values (**a**) and aeration modes (**b**).

As shown in Figure 10a, under a constant aeration pressure of 5 kPa, increasing the influent pH from 7.0 to 8.0 led to a progressive increase in AMO and HAO activities. Specifically, AMO activity increased from 31.82 ± 0.35 U·L^{-1} to 44.07 ± 0.28 U·L^{-1}, and HAO activity increased from 144.84 ± 3.15 U·L^{-1} to 200.45 ± 1.47 U·L^{-1}. In contrast, NXR activity decreased from 47.35 ± 0.34 U·L^{-1} to 43.23 ± 0.29 U·L^{-1} with the same pH increase. These results indicate that higher pH favors the conversion of ammonium to nitrite by enhancing AMO and HAO activities while slightly suppressing NXR activity.

Figure 10b shows the enzyme activities under different aeration modes at pH 8.0. Compared to constant aeration, both intermittent aeration and zero-pressure aeration resulted in decreased activities of all three enzymes. AMO activity decreased to 38.50 ± 0.53 U·L^{-1} (intermittent) and 38.30 ± 0.66 U·L^{-1} (zero-pressure). HAO activity decreased to 182.77 ± 0.92 U·L^{-1} and 182.81 ± 2.26 U·L^{-1}, respectively. NXR activity decreased to 41.52 ± 0.19 U·L^{-1} under intermittent aeration and further to 39.92 ± 0.32 U·L^{-1} under zero-pressure aeration.

Notably, AMO and HAO activities showed little difference between intermittent and zero-pressure aeration, which may explain why AOB can rapidly recover their activity even after prolonged oxygen limitation. In contrast, NXR activity continued to decline under oxygen-limiting conditions, consistent with the observed decrease in *Nitrospira* abundance and the progressive suppression of nitrite oxidation.

Taken together, these enzyme activity data provide direct functional evidence that the accumulation of nitrite under zero-pressure aeration is associated with reduced NXR activity. The suppression of NXR, combined with the relatively maintained AMO/HAO activities, contributes to the successful establishment of partial nitritation.

4. Conclusions

This study investigated the feasibility and microbial mechanisms of PN in a MABR under zero-pressure aeration. Zero-pressure aeration, requiring no external air supply, achieved stable PN with high nitrite accumulation. The underlying mechanism involves

selective suppression of NOB under extremely low dissolved oxygen conditions, as evidenced by decreased NXR activity and a modest shift in microbial community composition favoring AOB. Additionally, the increase in EPS, particularly protein components, reflected biofilm adaptation to nitrite-induced stress. The passive aeration strategy demonstrated in this study offers an energy-efficient and operationally simple alternative to conventional aeration control methods and is particularly attractive for decentralized or energy-limited wastewater treatment applications.

Supplementary Materials: The following supporting information can be downloaded at: https://www.mdpi.com/article/10.3390/environments13050264/s1, Text S1: Synthetic wastewater; Text S2: Analysis method. Figure S1: 3D-EEM fluorescence spectra of EPS in reactor: LB-EPS (a–c) and TB-EPS (d–f) at influent pH values of 7.0, 7.5, and 8.0; Figure S2: 3D-EEM fluorescence spectra of EPS in biofilm: LB-EPS (a–c) and TB-EPS (d–f) under constant, intermittent, and zero-pressure aeration. Table S1: The properties of the PDMS membrane used in this study; Table S2: The operating parameters of each stage during the start-up of the partial nitritation reactor.

Author Contributions: P.Y.: Writing—original draft, Software, Formal analysis, Y.C.: Formal analysis, Data curation. P.Z.: Writing—review and editing, Supervision, Project administration, Methodology, Conceptualization. Y.L.: View & Editing. M.Z.; View & Editing. H.Z.: View & Editing. S.P.: View & Editing. All authors have read and agreed to the published version of the manuscript.

Funding: This research is funded by National Natural Science Foundation of China (52500040), Basic Research Program of Jiangsu (BK20250618) and Natural Science Research of the Jiangsu Higher Education Institutions of China (25KJB610008). And The APC was funded by [Jiangsu (BK20250618)].

Data Availability Statement: The original contributions presented in this study are included in the article/Supplementary Materials. Further inquiries can be directed to the corresponding author.

Conflicts of Interest: The authors declare that they have no known competing financial interests or personal relationships that could have appeared to influence the work reported in this paper.

References

1. Wang, Y.; Zhu, T.; Chang, M.; Jin, D. Performance of a hybrid membrane aerated biofilm reactor (H-MBfR) for shortcut nitrification. *Biochem. Eng. J.* **2021**, *173*, 108089. [CrossRef]
2. Chang, M.; Liang, B.; Zhang, K.; Wang, Y.; Jin, D.; Zhang, Q.; Hao, L.; Zhu, T. Simultaneous shortcut nitrification and denitrification in a hybrid membrane aerated biofilms reactor (H-MBfR) for denitrification from low COD/N wastewater. *Water Res.* **2021**, *211*, 118027. [CrossRef]
3. Pellicer-Nacher, C.; Sun, S.; Lackner, S.; Terada, A.; Schreiber, F.; Zhou, Q.; Smets, B.F. Sequential aeration of membrane aerated biofilm reactors for high rate autotrophic denitrification: Experimental demonstration. *Environ. Sci. Technol.* **2010**, *44*, 7628–7634. [CrossRef]
4. Li, P.; Zhao, D.; Zhang, Y.; Sun, L.; Liu, J.; Wang, H.; Chen, X.; Wu, Q. Oil-field wastewater treatment by hybrid membrane-aerated biofilm reactor (MABR) system. *Chem. Eng. J.* **2015**, *264*, 595–602. [CrossRef]
5. Wei, X.; Li, B.; Zhao, S.; Qiang, C.; Zhang, H.; Wang, S. COD and nitrogen removal in facilitated transfer membrane-aerated biofilm reactor (FT-MABR). *J. Membr. Sci.* **2012**, *389*, 257–264. [CrossRef]
6. Mei, X.; Guo, Z.; Liu, J.; Bi, S.; Li, P.; Wang, Y.; Shen, W.; Yang, Y.; Wang, Y.; Xiao, Y.; et al. Treatment of formaldehyde wastewater by a membrane-aerated biofilm reactor (MABR): The degradation of formaldehyde in the presence of the cosubstrate methanol. *Chem. Eng. J.* **2019**, *372*, 673–683. [CrossRef]
7. Li, T.; Liu, J.; Bai, R.; Wong, F.S. Membrane aerated biofilm reactor for the treatment of acetonitrile wastewater. *Environ. Sci. Technol.* **2008**, *42*, 2099–2104. [CrossRef] [PubMed]
8. Liu, C.; Gong, P.F.; Xiao, T.M.; Zhang, M.; Nian, Y.J.; Yang, J.L.; Zhang, J. Atrazine wastewater treatment in a SPG membrane-aerated genetically engineered microorganism biofilm reactor. *Huanjing Kexue* **2014**, *35*, 3018–3023.
9. Vesuwe, R.N.; Nabaterega, R.; Ukaigwe, S.; Iorhemen, O.T. A systematic review of nitrogen removal pathways in membrane aerated biofilm reactor (MABR) systems. *J. Water Process Eng.* **2025**, *68*, 106502. [CrossRef]
10. Pellicer-Nàcher, C.; Domingo-Félez, C.; Lackner, S.; Smets, B.F. Microbial activity catalyzes oxygen transfer in membrane-aerated nitritating biofilm reactors. *J. Membr. Sci.* **2013**, *446*, 465–471. [CrossRef]

11. Chen, Y.; Zhao, Z.; Liu, H.; Ma, Y.; An, F.; Huang, J.; Shao, Z. Achieving stable two-stage mainstream partial-nitrification/anammox (PN/A) operation via intermittent aeration. *Chemosphere* **2020**, *245*, 125650. [CrossRef]
12. Chen, R.; Cao, S.; Zhang, L.; Zhou, Y. NOB suppression strategies in a mainstream membrane aerated biofilm reactor under exceptionally low lumen pressure. *Chemosphere* **2022**, *290*, 13338. [CrossRef] [PubMed]
13. Park, S.; Bae, W.; Chung, J.; Baek, S.C. Empirical model of the pH dependence of the maximum specific nitrification rate. *Process Biochem.* **2007**, *42*, 1671–1676. [CrossRef]
14. Fumasoli, A.; Morgenroth, E.; Udert, K.M. Modeling the low pH limit of Nitrosomonas eutropha in highstrength nitrogen wastewaters. *Water Res.* **2015**, *83*, 161–170. [CrossRef]
15. Zheng, M.; Wu, S.; Zuo, Z.; Wang, Z. Predictions of the influent and operational conditions for partial nitritation with a model incorporating pH dynamics. *Environ. Sci. Technol.* **2018**, *52*, 6457–6465. [CrossRef]
16. Niu, C.; Ying, Y.; Zhao, J.; Zheng, M.; Guo, J.; Yuan, Z.; Hu, S.; Liu, T. Superior mainstream partial nitritation in an acidic membrane-aerated biofilm reactor. *Water Res.* **2024**, *257*, 121692. [CrossRef]
17. Wang, L.; Zhang, C.; Kang, X.; Liu, Y.; Qiu, Y. Establishing mainstream partial nitrification in the membrane aerated biofilm reactor by limiting the oxygen concentration in the biofilm. *Water Res.* **2024**, *261*, 121984. [CrossRef] [PubMed]
18. Su, C.; Zheng, P.; Lin, X.; Chen, W.; Li, X.; Chen, Q.; Wu, S.; Chen, M. Influence of amoxicillin after pre-treatment on the extracellular polymeric substances and microbial community of anaerobic granular sludge. *Bioresour. Technol.* **2019**, *276*, 81–90. [CrossRef]
19. Xu, H.; Wang, C.; Liang, Z.; He, L.; Wu, W. The structure and component characteristics of partial nitrification biofilms under autotrophic and heterotrophic conditions. *Appl. Microbiol. Biotechnol.* **2015**, *99*, 3673–3683. [CrossRef]
20. Chen, W.; Westerhoff, P.; Leenheer, J.A.; Booksh, K. Fluorescence excitation-emission matrix regional integration to quantify spectra for dissolved organic matter. *Environ. Sci. Technol.* **2003**, *37*, 5701–5710. [CrossRef]
21. Xie, J.; Xin, X.; Ai, J.; Dong, W.; Zhang, S.; Li, J.; Wang, L. Synergic role of ferrate and nitrite for triggering waste activated sludge solubilisation and acidogenic fermentation: Effectiveness evaluation and mechanism elucidation. *Water Res.* **2022**, *226*, 119287. [CrossRef]
22. Liu, H.; Yang, F.; Shi, S.; Liu, X. Effect of COD/N ratio on denitrification in a membrane-aerated biofilm reactor. *Int. Biodeterior. Biodegrad.* **2016**, *113*, 74–79. [CrossRef]
23. Hartop, K.R.; Sullivan, M.J.; Giannopoulos, G.; Gates, A.J.; Bond, P.L.; Yuan, Z.; Clarke, T.A.; Rowley, G.; Richardson, D.J. The metabolic impact of extracellular nitrite on aerobic metabolism of *Paracoccus denitrificans*. *Water Res.* **2017**, *113*, 207–214. [CrossRef] [PubMed]
24. Wilén, B.M.; Lumley, D.; Mattsson, A.; Mino, T. Relationship between floccomposition and flocculation and settling properties studied at a full scale activated sludge plant. *Water Res.* **2008**, *42*, 4404–4418. [CrossRef]
25. Li, J.; Ye, W.; Wei, D.; Liu, T.; Zhang, Q.; Chen, W.; Li, J. System performance and microbial community succession in a partial nitrification biofilm reactor in response to salinity stress. *Bioresour. Technol.* **2018**, *270*, 512–518. [CrossRef] [PubMed]
26. Sun, Z.; Li, Y.; Li, M.; Wang, N.; Liu, J.; Guo, H.; Li, B. Steel pickling rinse wastewater treatment by two-stage MABR system: Reactor performance, extracellular polymeric substances (EPS) and microbial community. *Chemosphere* **2022**, *304*, 134402. [CrossRef]
27. Kornabos, M.; Dokianakis, S.N.; Lyberatos, G. Partial nitrification/denitrification can be attributed to the slow response of nitrite oxidizing bacteria to periodic anoxic disturbances. *Environ. Sci. Technol.* **2010**, *44*, 7245–7253. [CrossRef]
28. Pitol, C.S.; Fernandes, A.; Menegon, C.G. Enhancing deammonification in a membrane-aerated biofilm reactor: Intermittent aeration and ammonia loading rate control as key strategies for NOB inhibition in low-strength nitrogen wastewater. *J. Water Process Eng.* **2025**, *79*, 108861. [CrossRef]
29. Rosso, D.; Larson, L.E.; Stenstrom, M.K. Aeration of large-scale municipal wastewater treatment plants: State of the art. *Water Sci. Technol.* **2008**, *57*, 973–978. [CrossRef]
30. Ma, Y.; Peng, Y.; Wang, S.; Yuan, Z.; Wang, X. Achieving denitrification via nitrite in a pilot-scale continuous pre-denitrification plant. *Water Res.* **2009**, *43*, 563–572. [CrossRef]
31. Chen, R.; Zhou, Y. Mainstream nitrogen removal in membrane aerated biofilm reactor at minimal lumen pressure. *Sci. Total Environ.* **2022**, *818*, 151758. [CrossRef] [PubMed]
32. Zahedi, S.; Romero-Güiza, M.; Icaran, P.; Yuan, Z.; Pijuan, M. Optimization of free nitrous acid pre-treatment on waste activated sludge. *Bioresour. Technol.* **2018**, *252*, 216–220. [CrossRef]
33. Sijbesma, W.F.H.; Almeida, J.S.; Reis, M.A.M.; Santos, H. Uncoupling effect of nitrite during denitrification by Pseudomonas fluorescens: An in vivo P-NMR study. *Biotechnol. Bioeng.* **1996**, *52*, 176–182. [CrossRef]
34. Wett, B. Development and implementation of a robust deammonification process. *Water Sci. Technol.* **2007**, *56*, 81–88. [CrossRef]
35. Li, J.; Feng, M.; Zheng, S.; Zhao, W.; Xu, X.; Yu, X. The membrane aerated biofilm reactor for nitrogen removal of wastewater treatment: Principles, performances, and nitrous oxide emissions. *Chem. Eng. J.* **2023**, *460*, 141693. [CrossRef]

36. Wang, L.; Wang, Z.; Wang, F.; Li, M.; Zhang, Y.; Chen, R. Response of performance, antibiotic resistance genes and bacterial community exposure to compound antibiotics stress: Full nitrification to shortcut nitrification and denitrification. *Chem. Eng. J.* **2023**, *451*, 138750. [CrossRef]
37. Jiang, H.; Wang, Z.; Ren, S.; Qiu, J.; Li, X.; Peng, Y. Culturing sludge fermentation liquid-driven partial denitrification in two-stage Anammox process to realize advanced denitrification from mature landfill leachate. *J. Hazard. Mater.* **2021**, *415*, 125568. [CrossRef] [PubMed]
38. Zhang, H.; Gong, W.; Zeng, W.; Yan, Z.; Jia, B.; Li, G.; Liang, H. Organic carbon promotes algae proliferation in membrane-aeration based bacteria-algae symbiosis system (MA-BA). *Water Res.* **2020**, *176*, 115736. [CrossRef]
39. Chen, W.; Hu, F.; Li, X.; Yang, W.; Feng, S.; Yang, D.; Pang, W.; Lu, B. Deciphering the mechanism of medium size anammox granular sludge driving better denitrification performance. *Bioresour. Technol.* **2021**, *336*, 125317. [CrossRef]
40. van der Waals, M.J.; Plugge, C.; Meima-Franke, M.; de Waard, P.; Bodelier, P.L.; Smidt, H.; Gerritse, J. Ethyl tert-butyl ether (EtBE) degradation by an algal-bacterial culture obtained from contaminated groundwater. *Water Res.* **2019**, *148*, 314–323. [CrossRef]
41. Guadarrama, C.B.; Sanchez-Huerta, C.; Sanchez Medina, J.; Almulhim, F.; Hong, P.Y. Niche compartmentalization promotes dissolved methane removal and simultaneous nitrification and denitrification in a hybrid MABR. *Environ. Sci. Technol.* **2026**, *173*, 108089. [CrossRef]
42. Zhang, M.; Wang, Y.; Fan, Y.; Li, D.; Zhang, Y. Bioaugmentation of low C/N ratio wastewater: Effect of acetate and propionate on nutrient removal, substrate transformation, and microbial community behavior. *Bioresour. Technol.* **2019**, *306*, 122465. [CrossRef]
43. Liu, X.; Tang, P.; Liu, Y.; He, Y.; Zhang, B. Efficient removal of organic compounds from shale gas wastewater by coupled ozonation and moving-bed-biofilm submerged membrane bioreactor. *Bioresour. Technol.* **2022**, *344*, 126191. [CrossRef] [PubMed]
44. Li, Y.; Dong, R.; Guo, J.; Wang, L.; Zhao, J. Effects of Mn^{2+} and humic acid on microbial community structures, functional genes for nitrogen and phosphorus removal, and heavy metal resistance genes in wastewater treatment. *J. Environ. Manag.* **2022**, *313*, 115028. [CrossRef]
45. Ma, Y.; Domingo-Félez, C.; Plósz, B.G.; Smets, B.F. Intermittent aeration suppresses nitrite-oxidizing bacteria in membrane aerated biofilms: A model-based explanation. *Environ. Sci. Technol.* **2017**, *51*, 6145–6155. [CrossRef] [PubMed]
46. Wang, L.; Zhang, C.; Liu, Y.; Qiu, Y.; Wanyan, D.; Liu, J.; Cheng, G.; Lin, P.; Huang, X. *Achieving* mainstream nitrogen removal by partial nitrification and anammox in the carriers-coupled membrane aerated biofilm reactor. *Water Res.* **2024**, *271*, 123000. [CrossRef]

Disclaimer/Publisher's Note: The statements, opinions and data contained in all publications are solely those of the individual author(s) and contributor(s) and not of MDPI and/or the editor(s). MDPI and/or the editor(s) disclaim responsibility for any injury to people or property resulting from any ideas, methods, instructions or products referred to in the content.